ULATRAFAST LASERS FOR THE DETECTION AND QUANTITATION OF TRACE CRYSTALLINITY IN AMORPHOUS FORMULATIONS BY SONICC

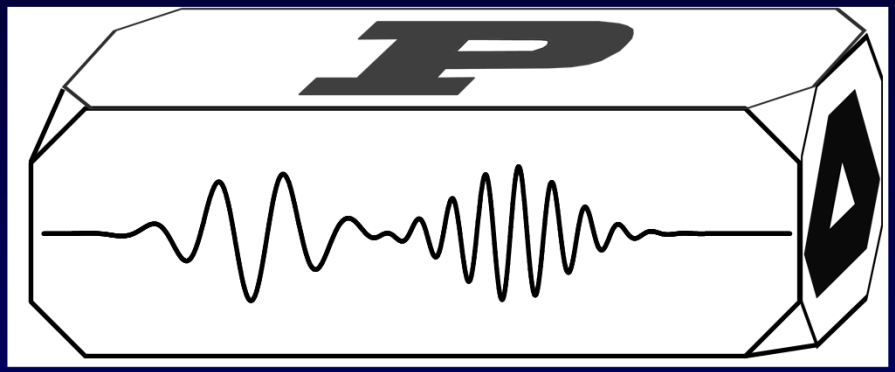

Garth J. Simpson

Department of Chemistry
Purdue University

This document was presented at PPXRD - Pharmaceutical Powder X-ray Diffraction Symposium

Sponsored by The International Centre for Diffraction Data

PPXRD Website – www.icdd.com/ppxrd

ICDD Website - www.icdd.com

The bipolar behavior of APIs

–Active pharmaceutical ingredients (APIs) must be both highly water-soluble to dissolve in the blood and gut, but sufficiently hydrophobic to pass through cell membranes.

–Modern drug discovery machinery is increasingly leading to more specific drug candidates with fewer side-effects and greater chemical complexity. The increase in molecular size exacerbates the challenges in solubility / dissolution.

–Roughly half of all promising API candidates are currently abandoned due to poor aqueous solubility.

The bipolar behavior of APIs

- Apart from chemical modification, little can be done to impact permeability.
- Formulations efforts are routinely dedicated to characterizing and addressing limitations from slow dissolution kinetics.

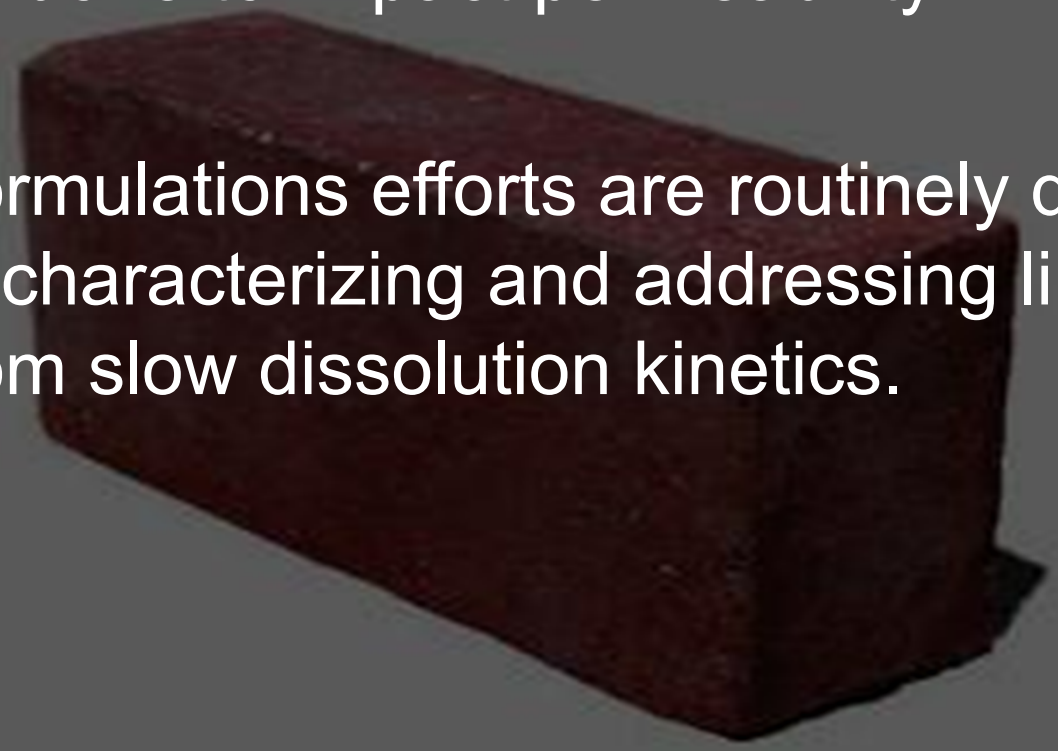

Common current methods for API solid state analysis

- Suite of common analysis tools for quantitative information on crystallization energetics and kinetics in complex matrices and powders:

Bright field microscopy	(fast, but not selective)
Raman microscopy	(selective, but not fast)
X-ray powder diffraction	(high detection limits, 1%)
Calorimetry	(high detection limits, 1-10%)
SEM	(usually not real-time)

- In amorphous formulations, the total drug loading may only be on the order of a few percent.

The Basic Tools:

One-photon excited fluorescence

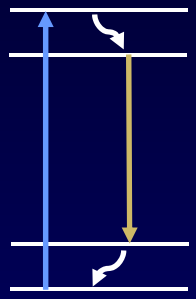

Reflection & birefringence

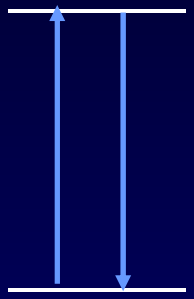

Linear Optics

TPEF: two-photon excited fluorescence

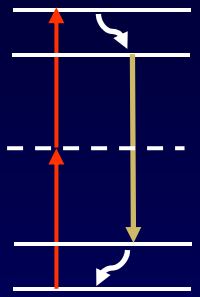

SHG: Second harmonic generation

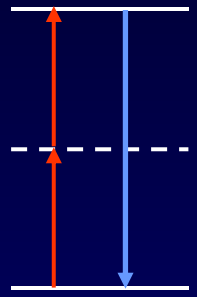

Nonlinear Optics (NLO)

Applications of SONICC and TPE-UVF in API Analysis

- Quantification of trace crystallinity within amorphous dispersions.
- Energetics of crystal nucleation and growth in powders and films.
- Accelerated stability studies.
- API distributions within final dosage forms.
- HT screening for API chiral resolution.
- Polymorph screening.

I. Classical 1D Model for Nonlinear Optics

In linear interactions describing reflection, refraction, and light-scattering, the driving field induces a polarization at the same frequency.

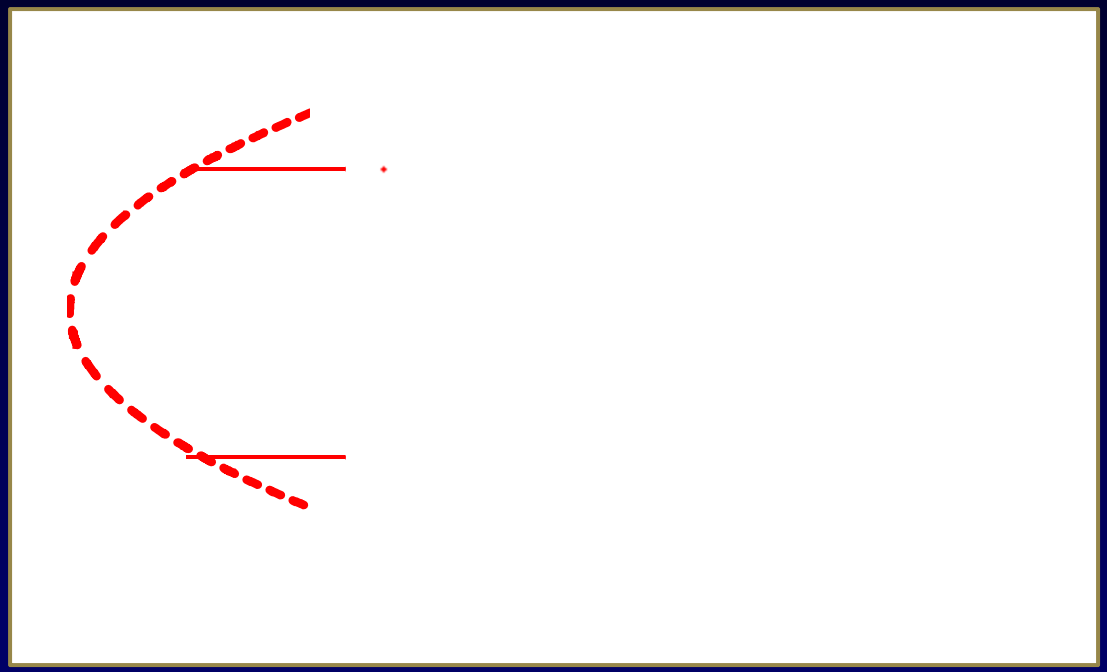

I. Classical 1D Model for Nonlinear Optics

When the field strength is increased, additional anharmonic contributions become significant, resulting in distortions in the induced polarization.

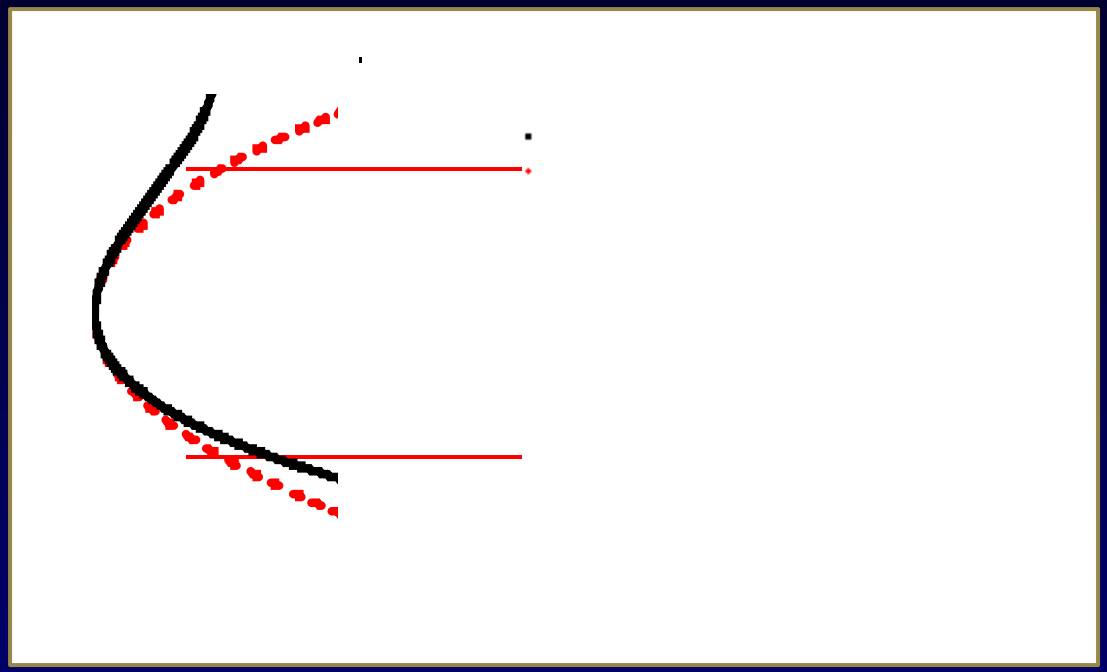

I. Classical 1D Model for Nonlinear Optics

These distortions in the time-domain are recovered in the frequency-domain by contributions at the higher harmonics.

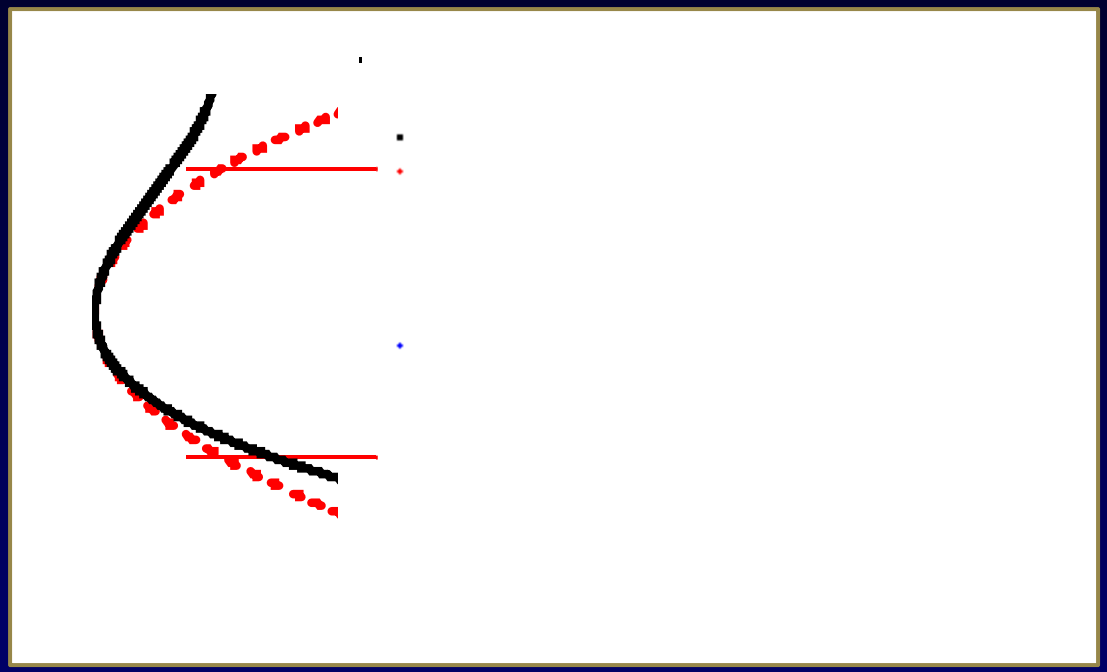

I. Classical 1D Model for Nonlinear Optics

The net polarization at the second harmonic frequency arises from the coherent interference of all “oscillators”.

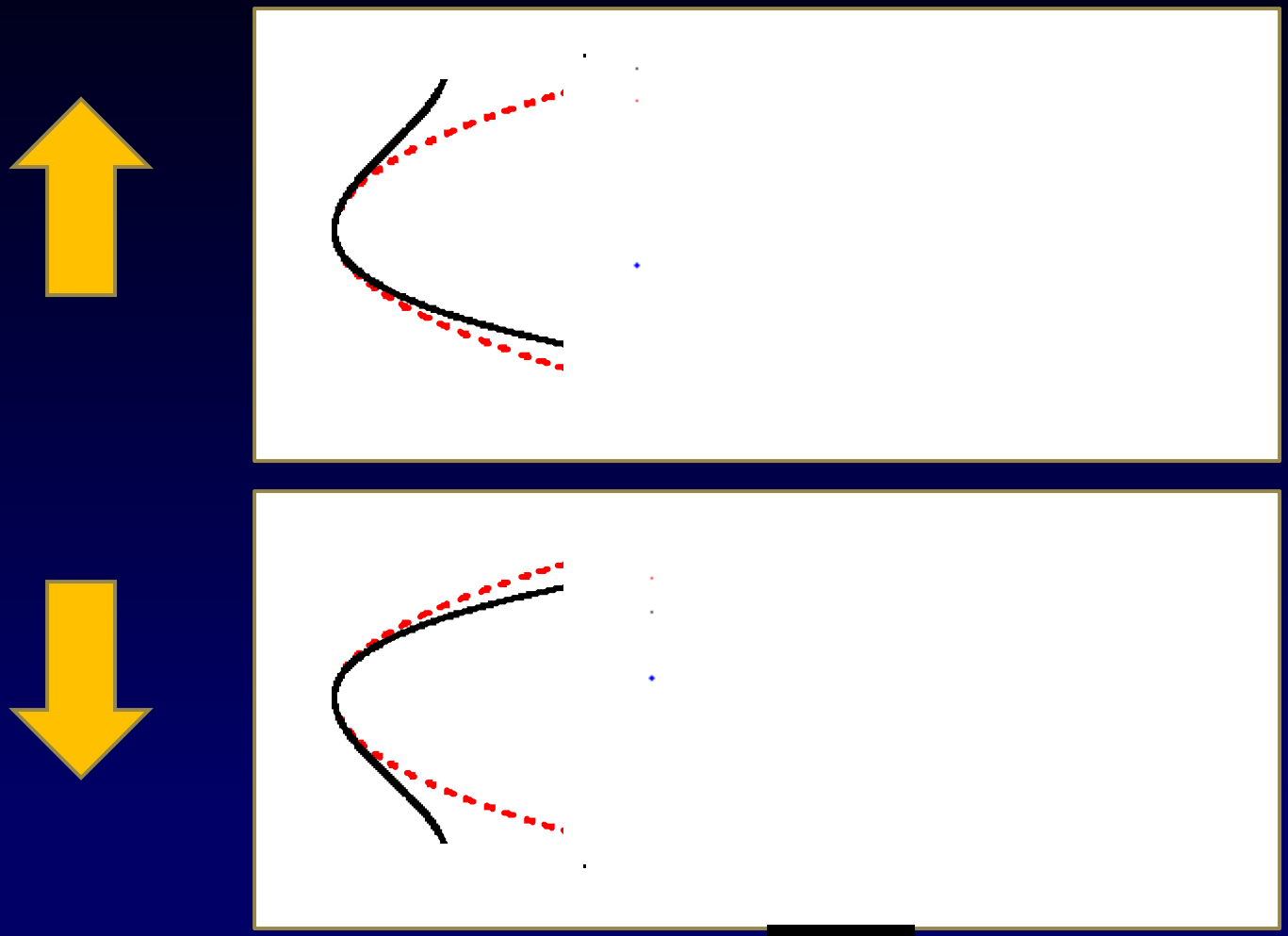

Second Order Nonlinear Optical Imaging of Chiral Crystals (SONICC)

Second Harmonic Generation (SHG)

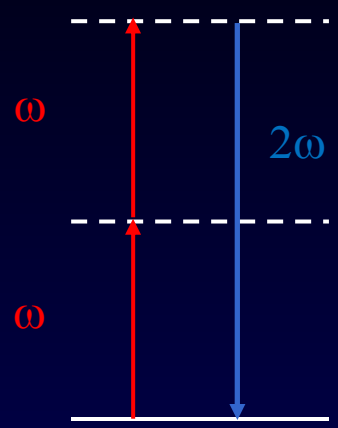

SHG is highly selective for ordered crystalline assemblies of chiral molecules i.e. crystals with *no inversion symmetry*.

Unordered media result in cancellation and generate no coherent SHG.

SHG active

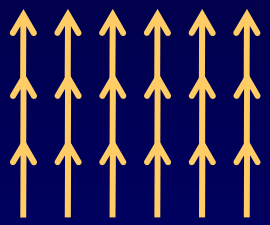

Chiral crystals

SHG inactive

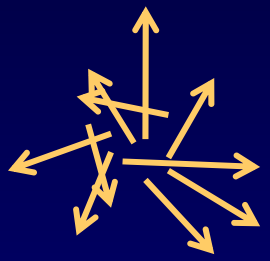

Liquid, glass, amorphous

Beam-Scanning SHG Microscopy

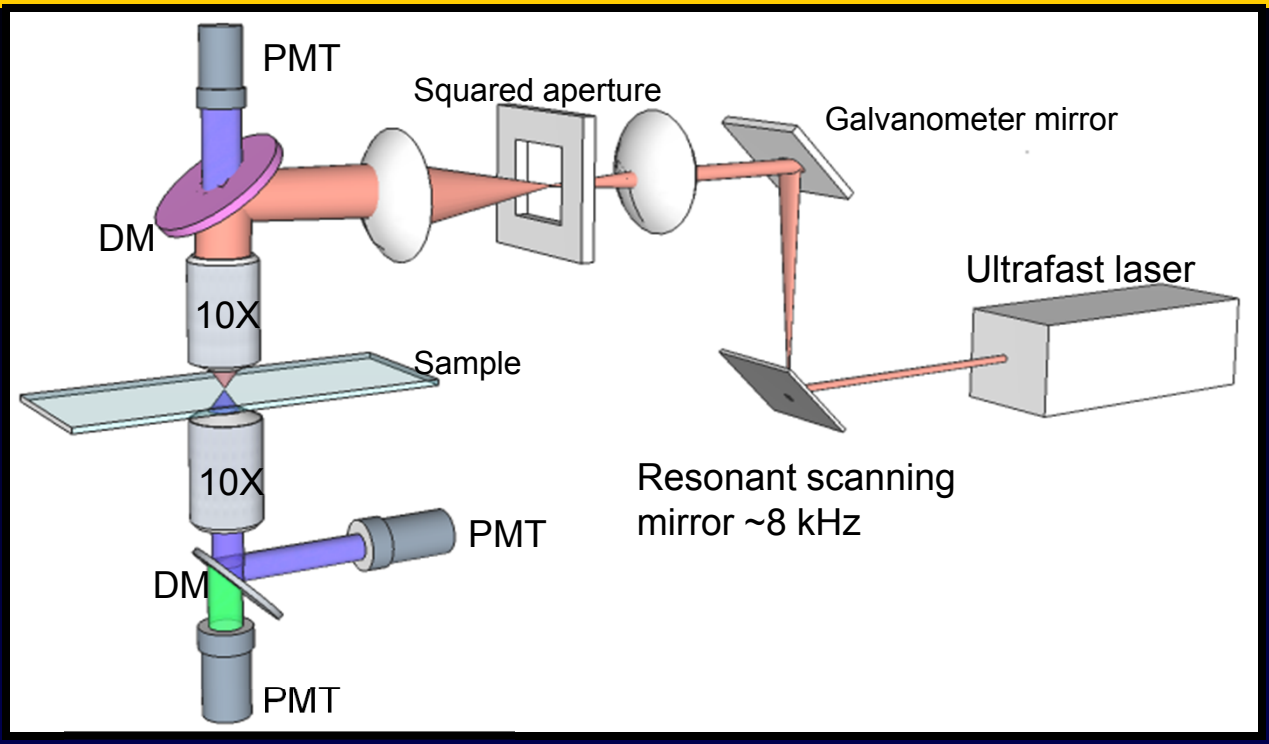

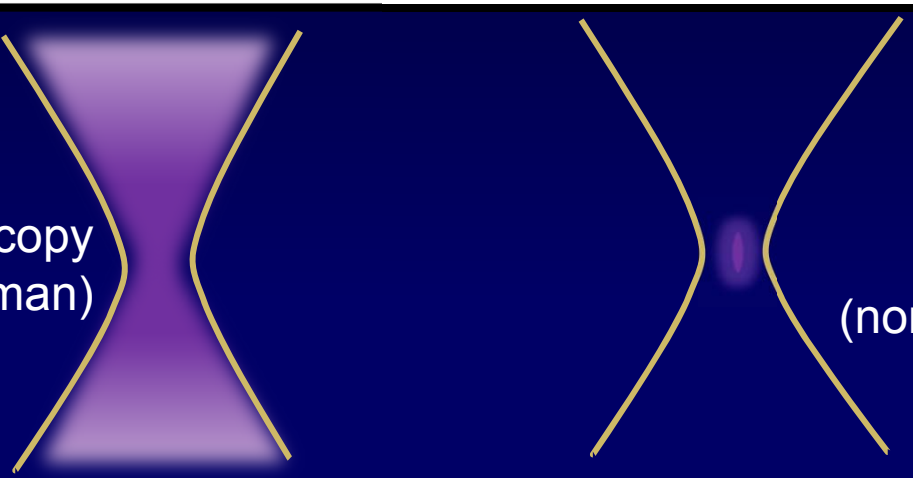

Linear microscopy
(including Raman)

SONICC
TPE-UVF
(nonlinear microscopy)

II. Amorphous pure API films

- Raising an API above the melting temperature is the simplest route to generate amorphous materials.

II. Isothermal crystallization of amorphous griseofulvin, SONICC vs. bright-field

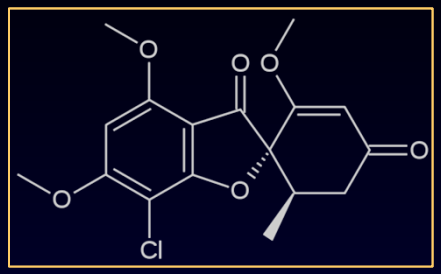

Space group : $P4_1$

SHG: threshold image

-melt-quenched griseofulvin
-45 s / frame, 50 mW, 800 nm, 100 fs at 80 MHz
-Threshold set at signal / bkg = 3

Crystallization of griseofulvin from an amorphous melt
no residual nuclei

SONICC

Bright field

50 μm

II. Isothermal crystallization of amorphous griseofulvin, SONICC vs. bright-field

Isothermal crystallization of griseofulvin at 128°C

In each experiment, SONICC yields

Nucleation kinetics

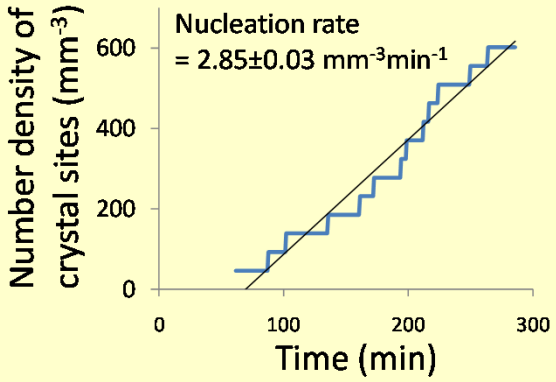

Single-crystallite kinetics

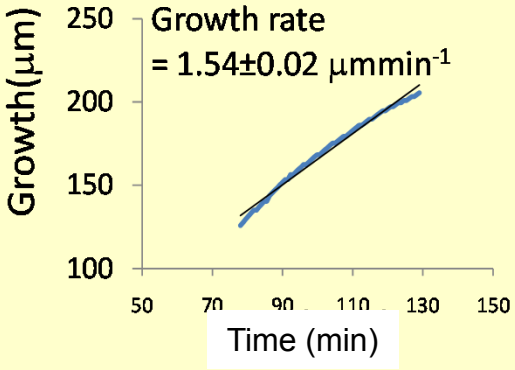

Macroscopic relative crystallinity

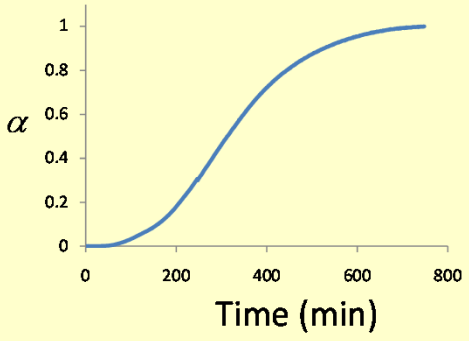

II. Isothermal crystallization of amorphous griseofulvin, SONICC vs. bright-field

Johnson-Mehl-Avrami (JMA) equation $\alpha(t) = 1 - e^{(-(k(t-t_0))^n)}$

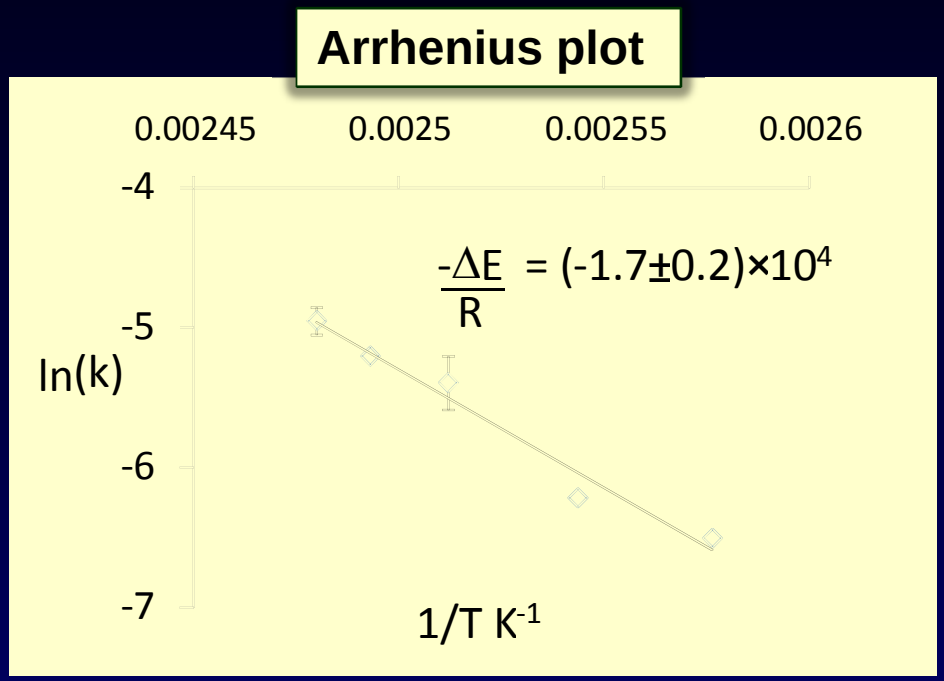

-SONICC yields a free energy barrier of 140±20 kJ/mol for crystal nucleation.

-Previous studies using thermal methods report a barrier of 167 kJ/mol.*

Avrami, M., *J. Chem. Phys.* **1939,** *7*, 1103-1112
Avrami, M., *J. Chem. Phys.* **1940,** *8*, 212-224
Avrami, M., *J. Chem. Phys.* **1941,** *9*, 177-184
Johnson, W.A..; Mehl, R. F., Trans. Am. Inst. Min. Metall. Eng. **1939,** *135*,416-442
*Zhou, D.; Zhang, G. G. Z.; Law, D.; Grant, D. J. W.; Schmitt, E. A. *Molecular Pharmaceutics* **2008**, *5*, 927-936.

Estimated detection limit of SONICC

SHG is a coherent process

Backward coherence length

$$L_C^b = \frac{\lambda}{4} \cdot \frac{1}{\left| n^{2\omega} + n^{\omega} \right|}$$

Forward coherence length

$$L_C^f = \frac{\lambda}{4} \cdot \frac{1}{\left| n^{2\omega} - n^{\omega} \right|}$$

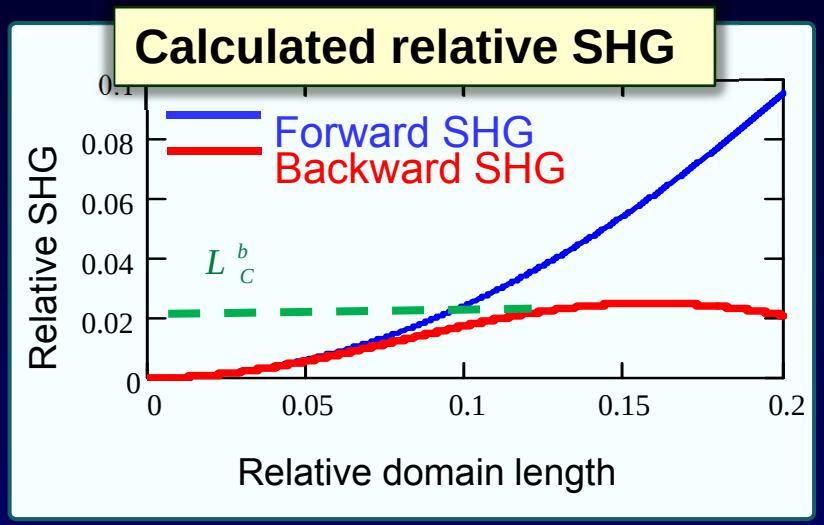

L_{bC}(griseofulvin)=120 nm

Smallest detectable crystal = 90 nm

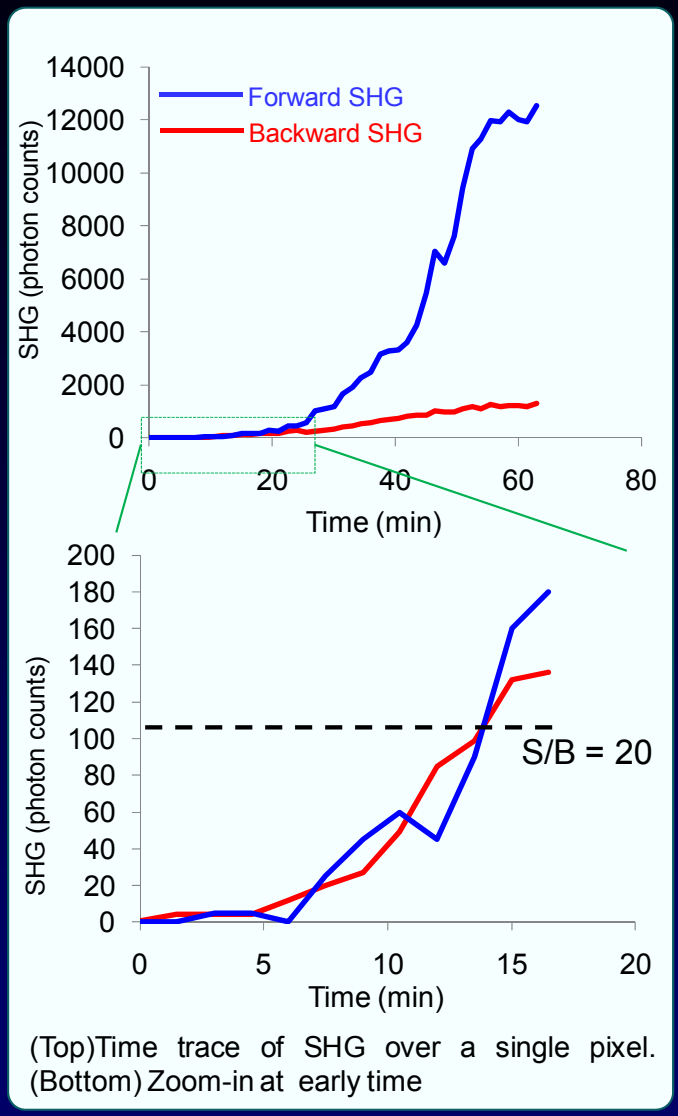

(Top)Time trace of SHG over a single pixel. (Bottom) Zoom-in at early time

Detection limits of ~3 ppt crystallinity.

~10^7-fold reduction compared to established methods.

III. Amorphous Solid Dispersions

- Target:
  - Quantification of trace crystallinity in amorphous solid dispersions.
  - Assessment of kinetics of crystal formation for accelerated stability studies.
  - Correlation between spatial distributions of APIs and crystallization/dissolution kinetics.

Quantitative Comparison with Raman and PXRD: NAP in PEG

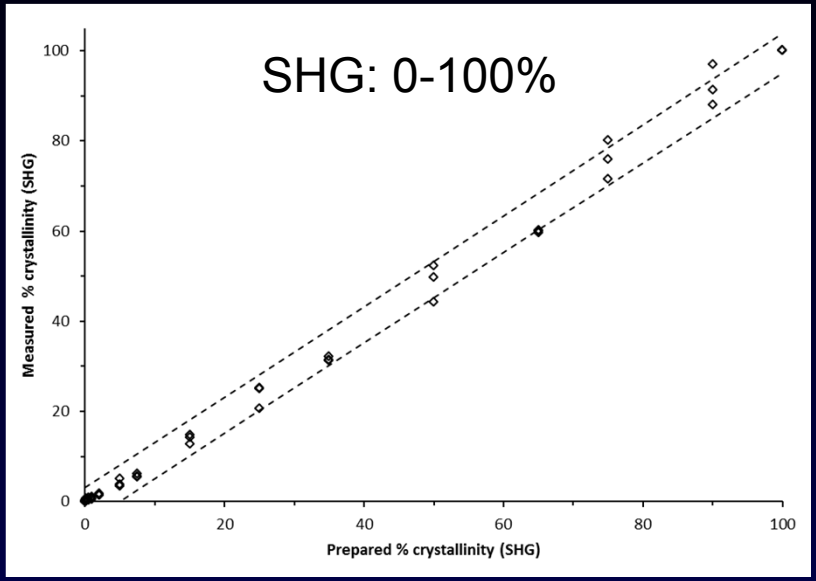

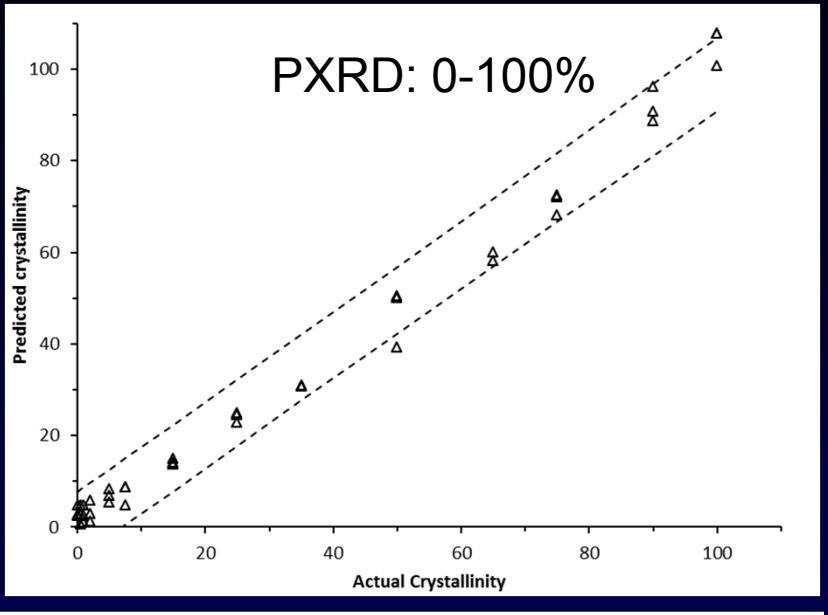

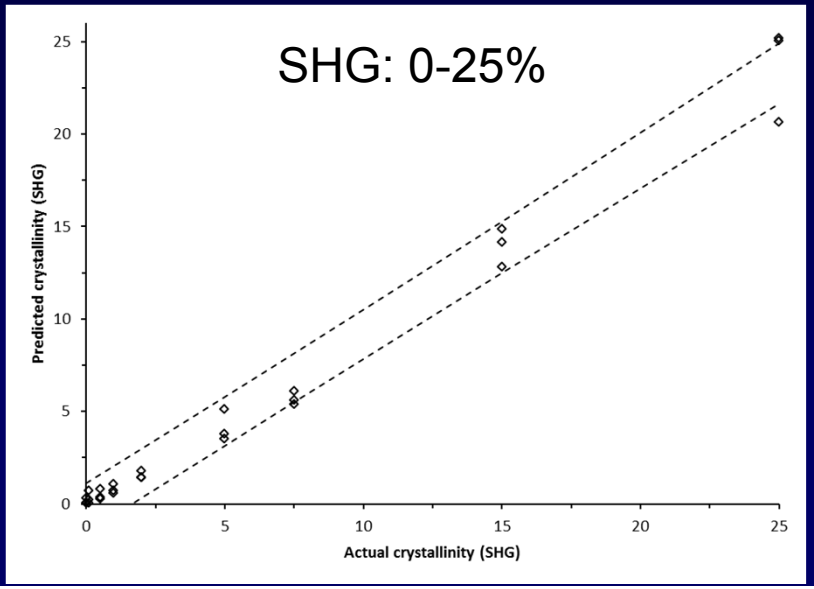

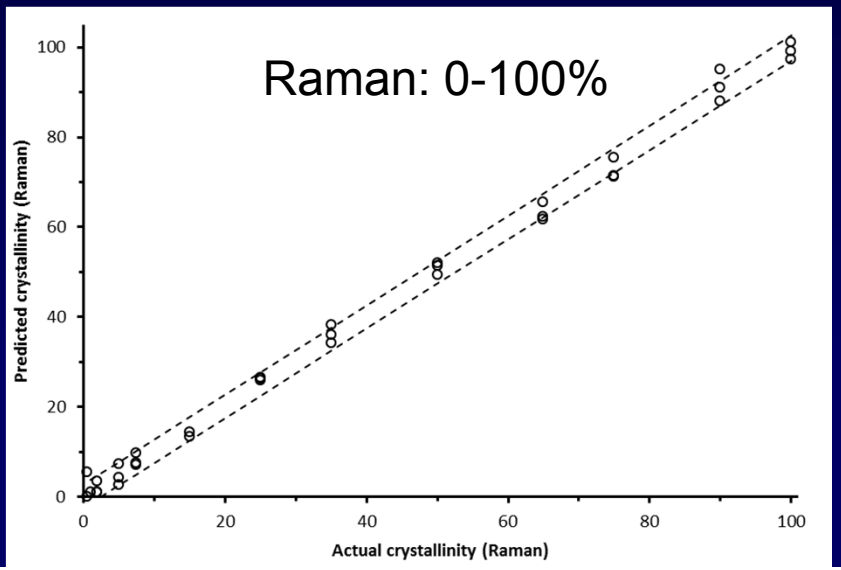

IV. Pure cryomilled powders

- Milling is among the oldest and most common methods for API preparation.
- Experimental observations have indicated a loss of crystallinity upon extensive milling of some APIs.
- The mechanism of action has not been definitively identified.

Single step $C \rightarrow A$

Multiple step $C \rightarrow c + c + c + c... \rightarrow A$

IV. Mechanism of Action of Cryomilling.

PXRD

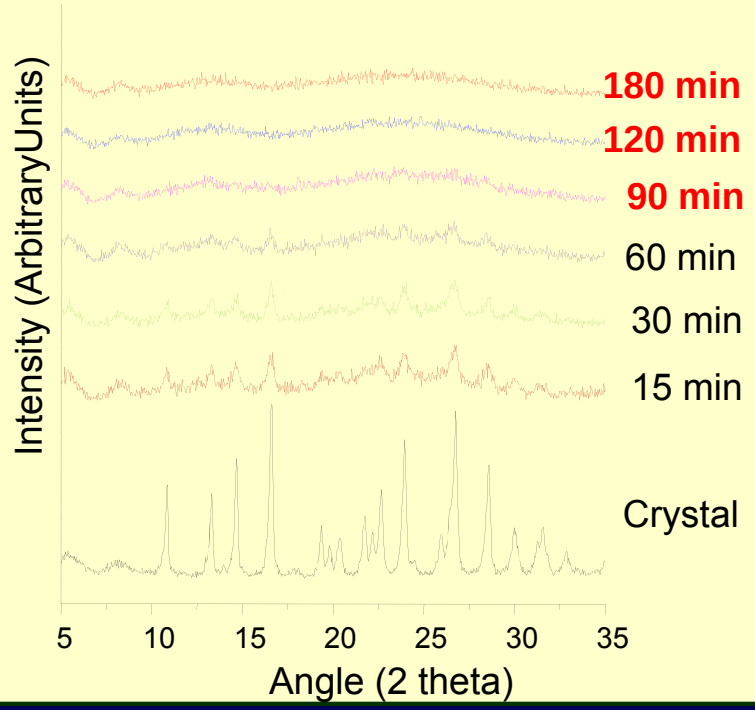

SONICC

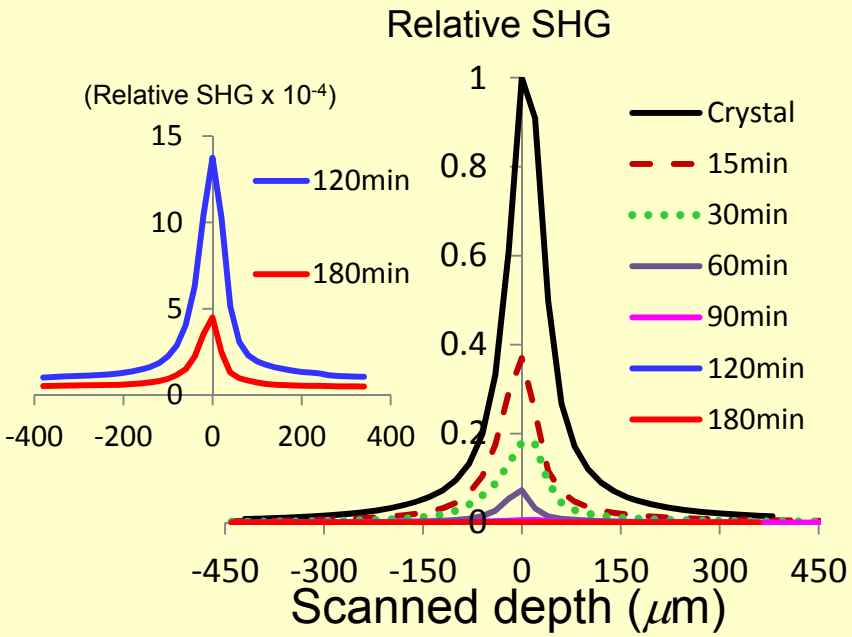

Cryomilled griseofulvin
-10Hz, 10 min/cycle
-particle (conglomerate) size range 50-150 μm

3-D SHG images of cryomilled griseofulvin

Macroscopic crystallinity arises from localized crystalline domains

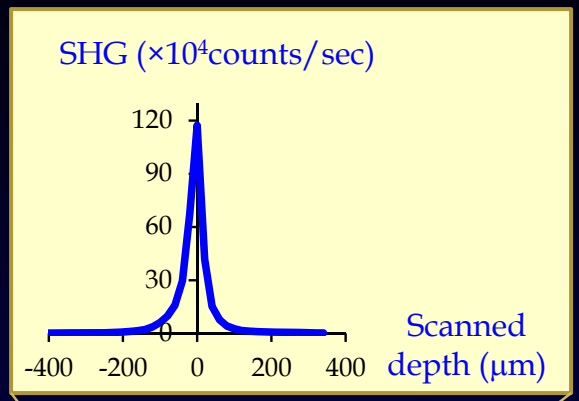

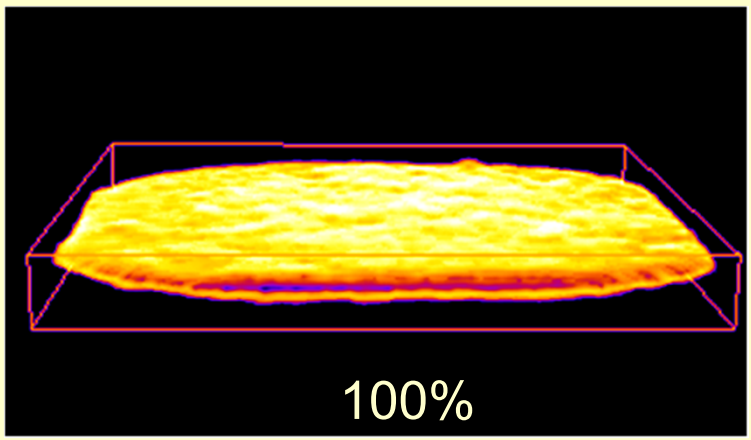

100%

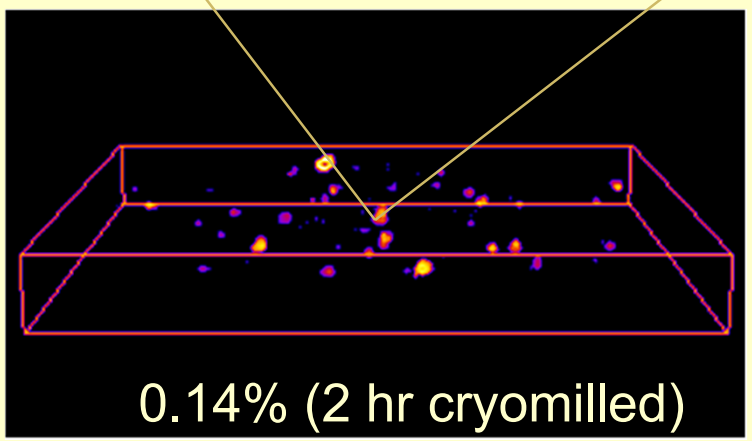

0.14% (2 hr cryomilled)

Residual crystallinity upon cryomilling (2)

Questions:

1. Is the powder truly amorphous?
2. What is the mechanism for the loss in crystallinity?

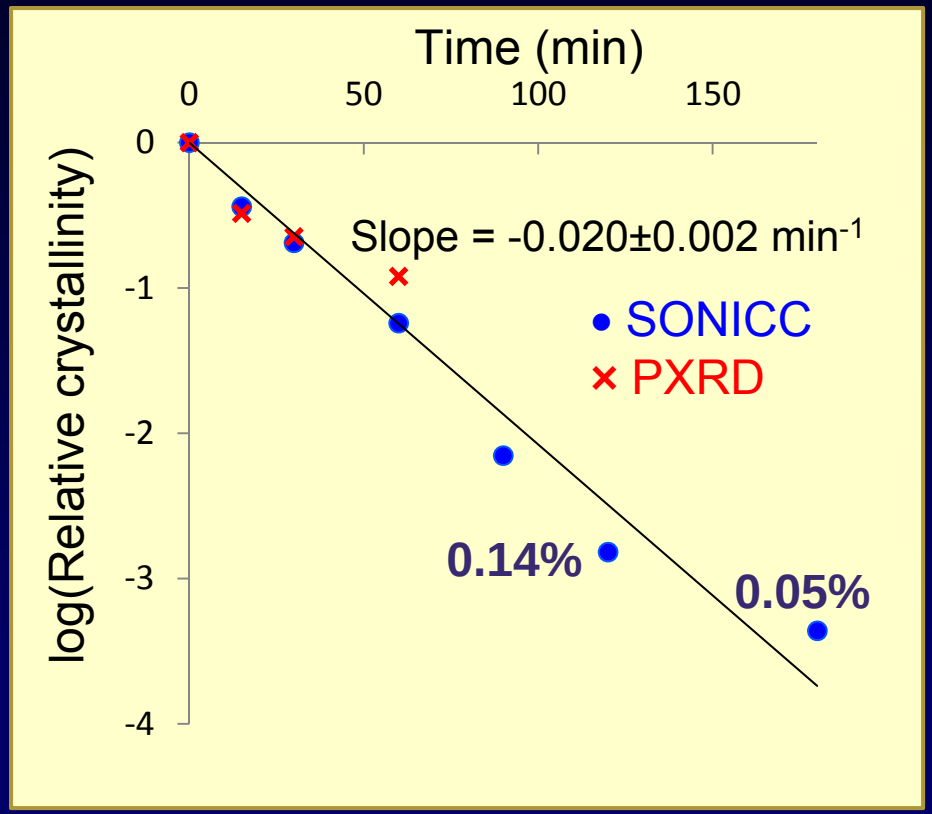

SONICC enables quantitation of crystallinity at least 3 decades lower than the PXRD.

Reduction of crystallinity upon cryomilling follows first order kinetics in milling time.

Crystal size distribution

Questions:

1. Is the powder truly amorphous?
2. What is the mechanism for the loss in crystallinity?

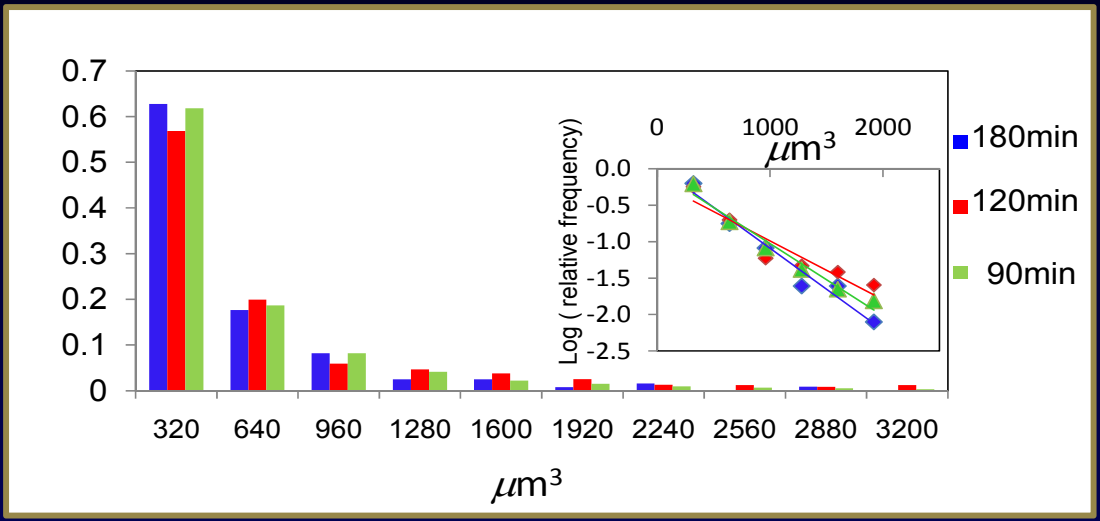

- Particle size distributions are constant after 90 minutes.
- Particles have reached their fracture limit prior to 90 minutes of milling.

Macroscopically, 1st order reduction of crystallinity was observed.

Single step $C \rightarrow A$

Multiple step $C \rightarrow c + c + c + c... \rightarrow A$

Nucleation rates in API powders

Direct determination of nucleation kinetics requires spatial information.

Optical microscopy is typically used for monitoring crystal nucleation rates within *transparent* media.

Although several methods are available for probing ensemble-averaged % crystallinity in powders, few routine methods are available for probing API nucleation kinetics in powders.

$$\text{Nucleation rate} = \frac{\Delta \text{ Number of crystals per unit volume}}{\Delta t}$$

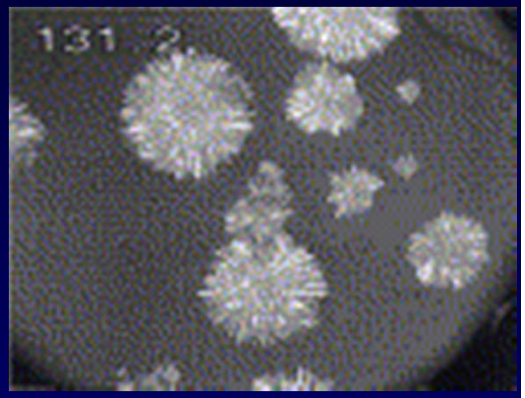

Andronis, V. and G. Zografi (2000). Journal of Non-Crystalline Solids **271(3): 236-248.**

Re-crystallization of griseofulvin

Isothermal crystallization at 50°C for 400 min

Cryomill

Melt-quench
(true glassy state)

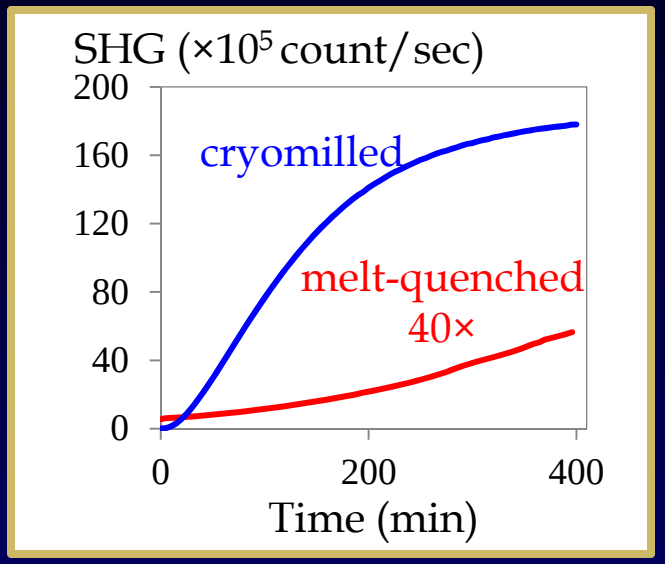

Summary of Results with Amorphous Formulations

- SONICC provides selective detection of chiral crystals in complex matrices with detection limits ~10^4 – fold lower than common benchtop alternatives.
- Comparisons with powder XRD and Raman demonstrate quantitative agreement between the different methods.
- Crystal size distributions and shape can dramatically impact crystallization kinetics in amorphous formulations.
- The mechanism of action of amorphous rendering via cryomilling was elucidated.

V. Direct Evidence for Ostwald Rule of Stages for Polymorph Transitioning

- Wilhelm Ostwald proposed a step-wise phase change at the early stages of adiabatic crystallization, in which initial metastable polymorphs eventually transition to the more thermodynamically stable forms.
- Direct evidence supporting Ostwald transitioning is complicated by the transient nature and small sizes routinely expected for the metastable polymorphs.

V. Classical Nucleation Theory

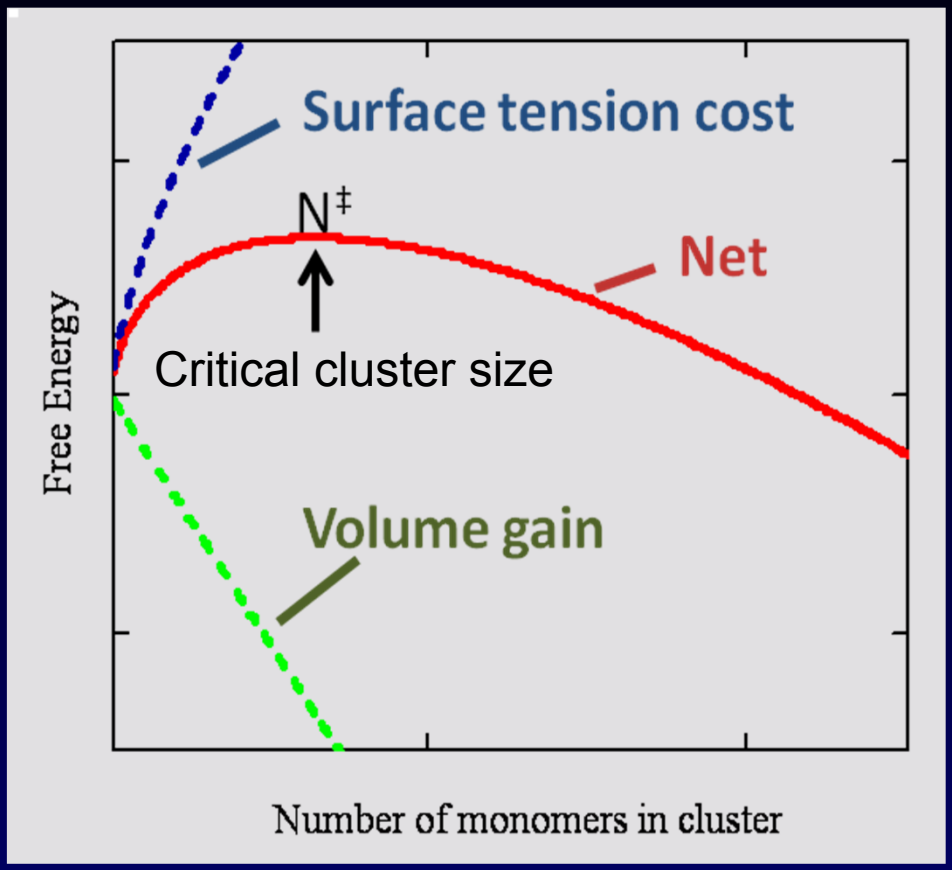

According to classical nucleation theory, the critical cluster size for crystal nucleation is dictated by the balance between the bulk free-energy benefit and the surface tension cost.

V. Classical Nucleation Theory

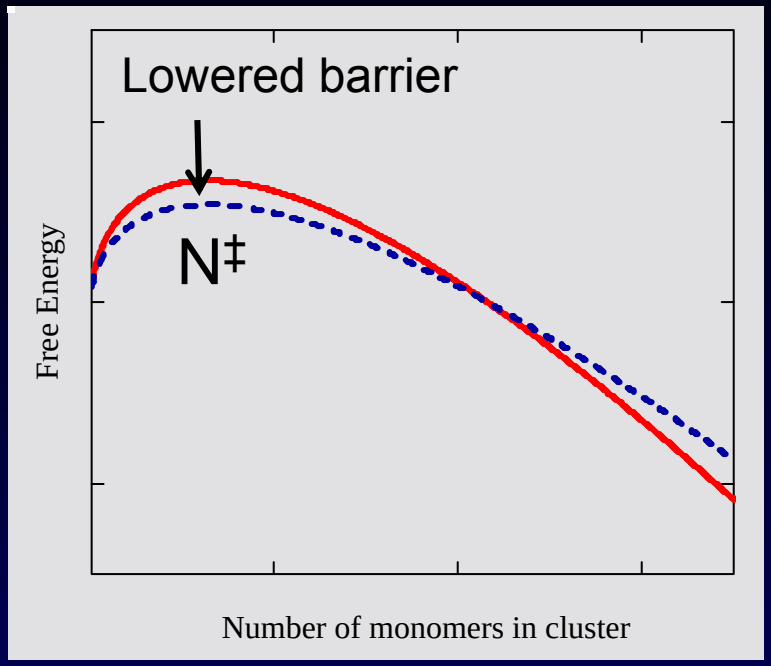

Barriers for nucleation can be lowered by initial nucleation of crystal polymorphs with reduced surface free-energy. Under appropriate conditions, crystallization may proceed through a series of 3D packing rearrangements.

-Ostwald, W. (1897) *Zeitschrift fur Physikalsche Chemie* **1897,** *22*, 289-330.

V. Preliminary Evidence: Racemic Amino Acid Solutions

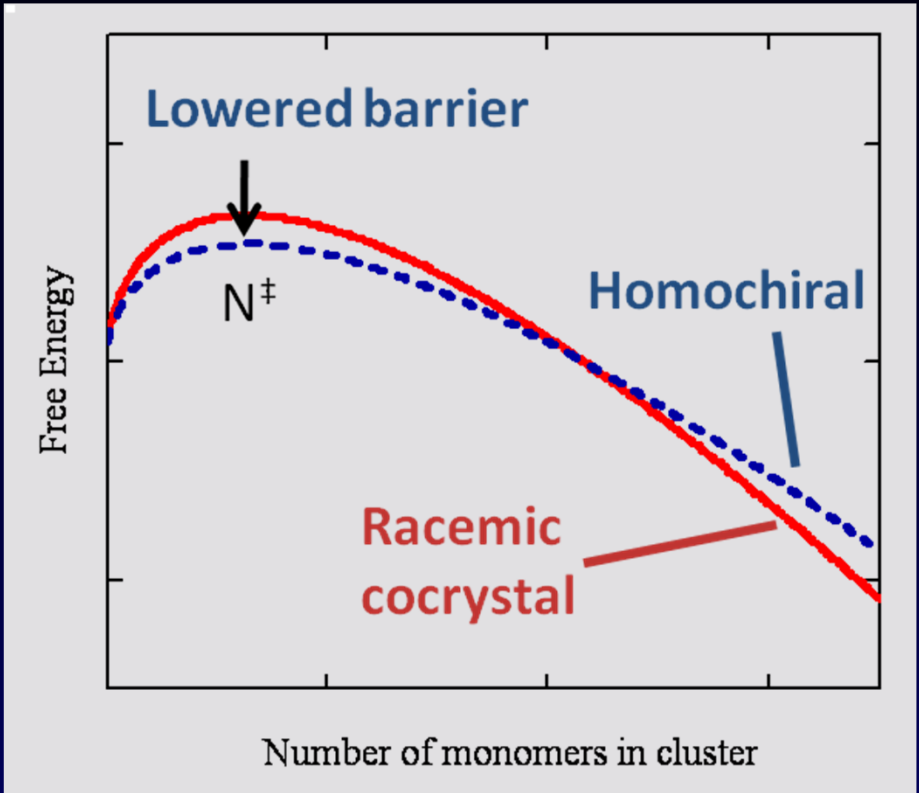

-In most instances, the racemic co-crystal is more energetically stable than a conglomeration of homochiral crystals.

-A large kinetic barrier is expected for transitioning from one form to the other because of the required mass transport involved.

SHG images acquired during drying of serine solutions.
(800 nm, 100 mW, 120 fs, 8s/frame)

Homochiral solution

Racemic solution

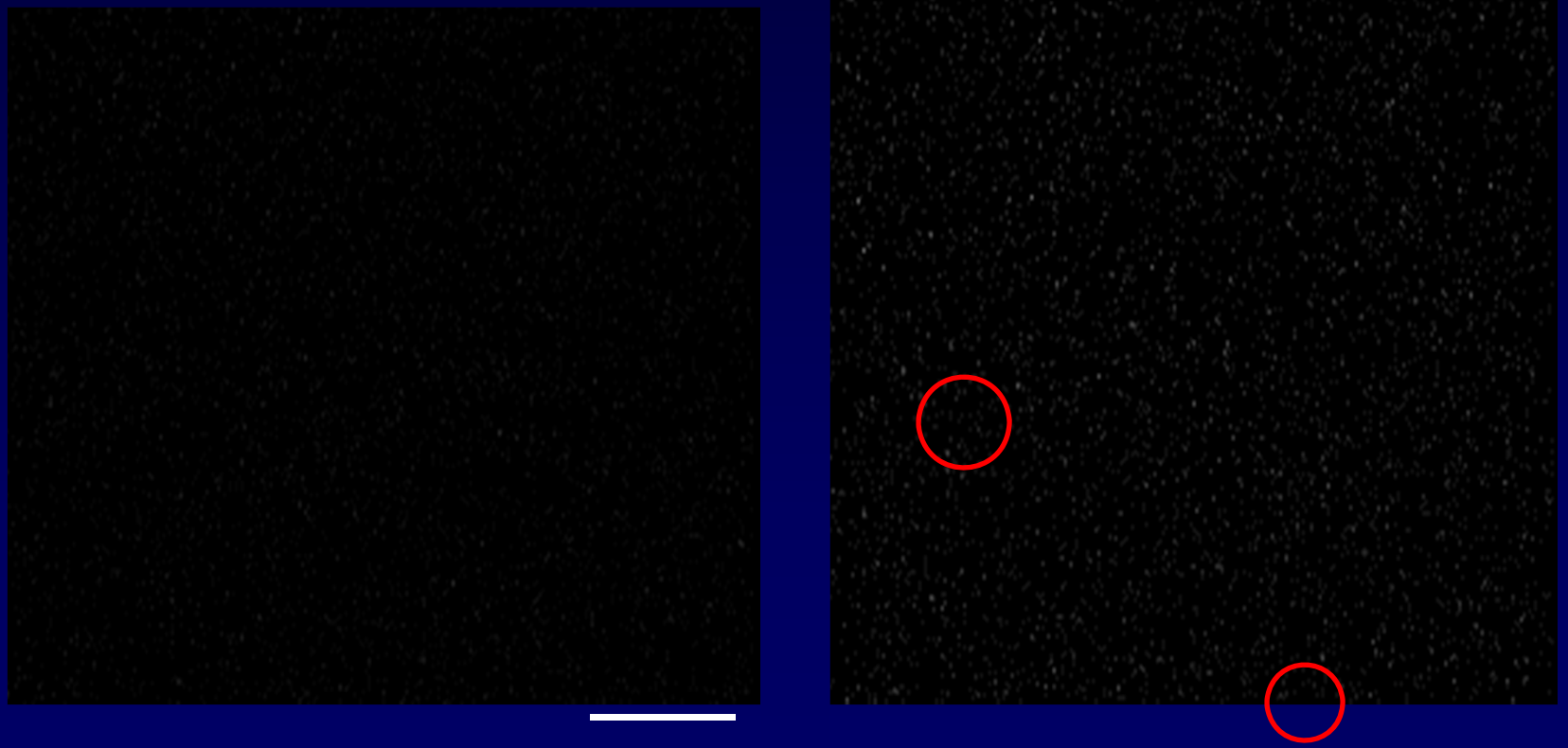

Time-traces demonstrate transient SHG-active regions during crystallization of the racemic solution.

Racemic solution

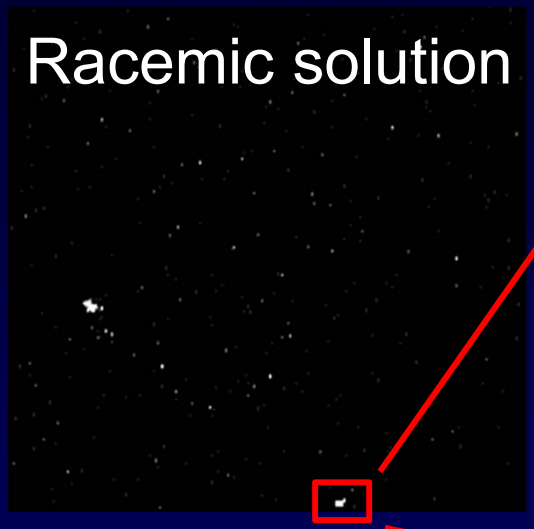

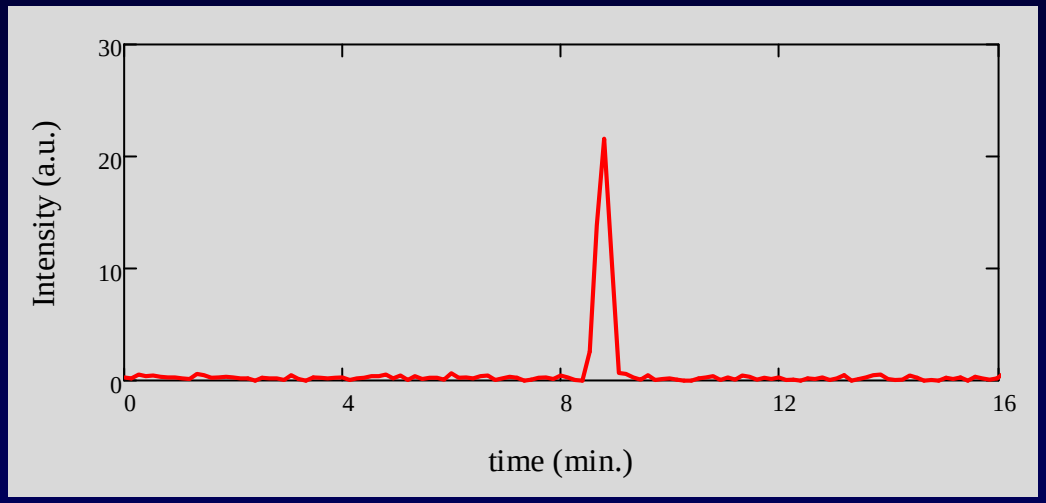

(D)-serine solution

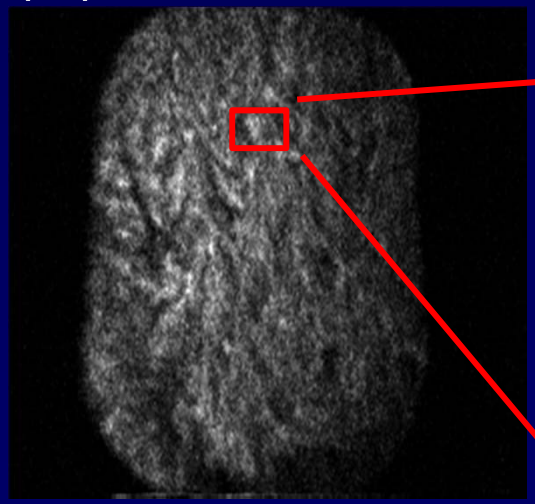

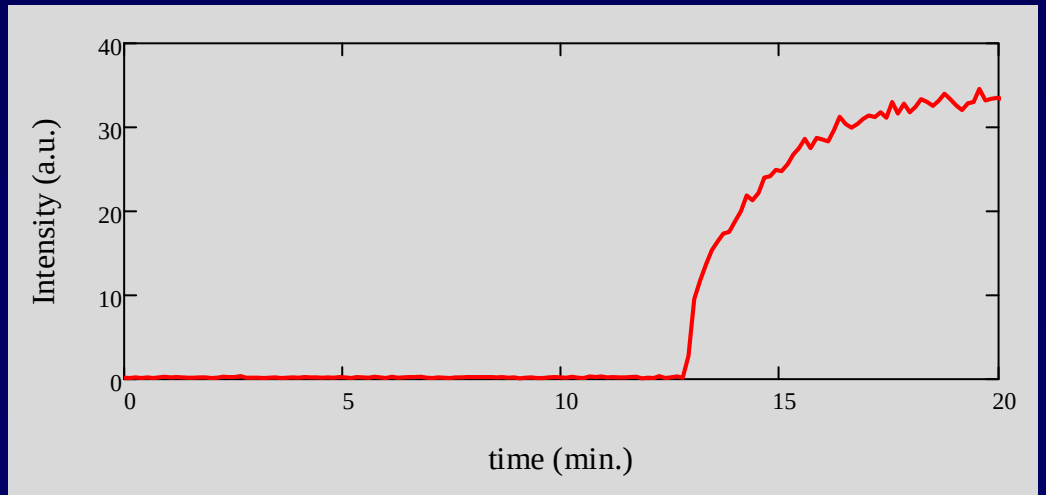

Rapid solvent evaporation also produces metastable polymorphs

Chemical inkjet printing of racemic amino acid solutions produces SHG-active spots from solutions that are dark upon slow solvent evaporation.

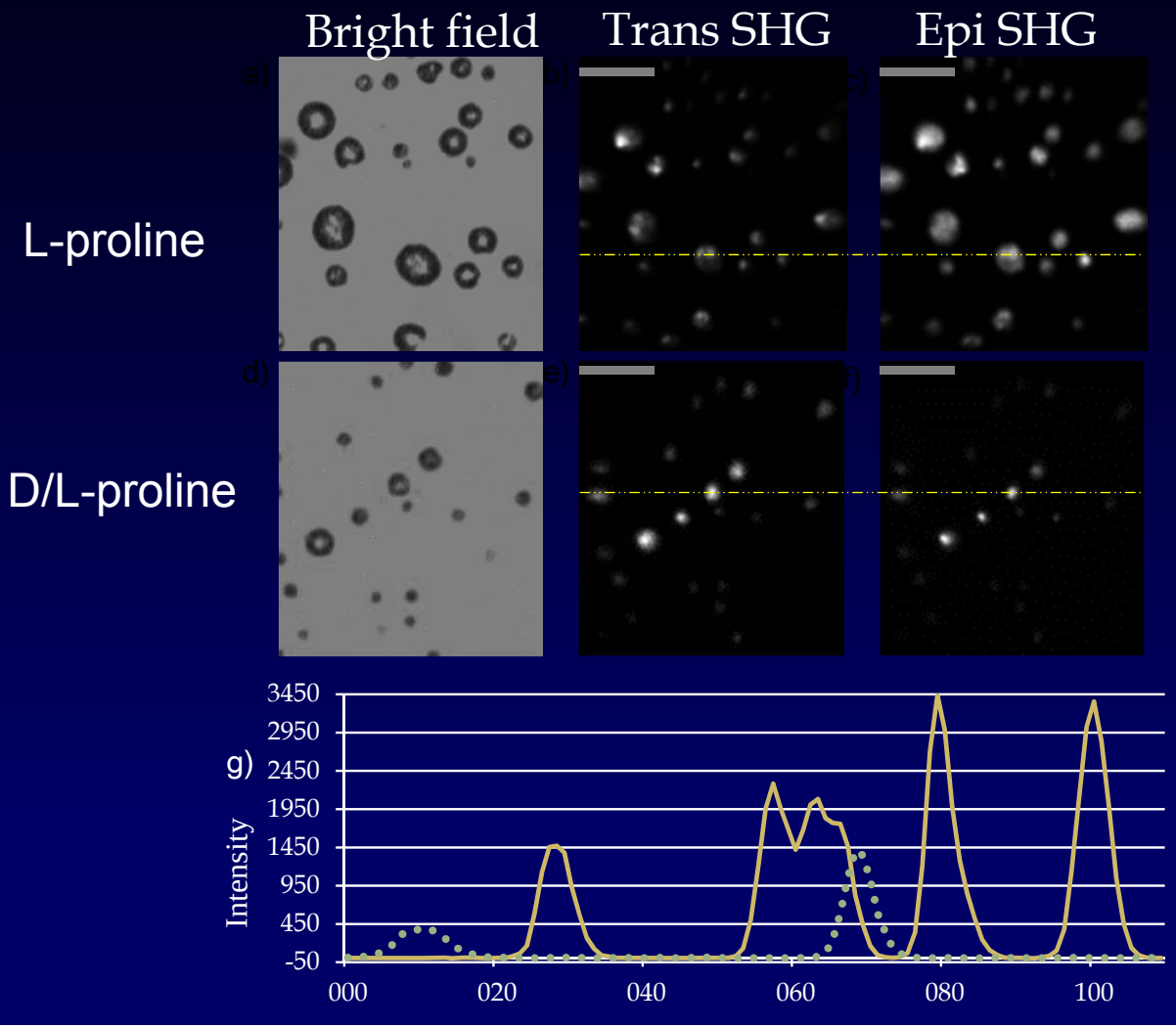

Acknowledgements

Purdue
Professor Lynne Taylor
Umesh Kestur
Qing Zhu

Merck
Patrick Marsac

Funding
•NSF
•Purdue Discovery Research Center
•Dane O. Kildsig Center of Pharmaceutical Processing Research